UC Irvine
UC Irvine Previously Published Works

Title

Chemical transport across the ITCZ in the central Pacific during an El Niño-Southern Oscillation cold phase event in March-April 1999

Permalink

Journal

ISSN

Authors

Avery, Melody A
Westberg, David J
Fuelberg, Henry E
et al.

Publication Date

DOI

Copyright Information

Peer reviewed

Chemical transport across the ITCZ in the central Pacific during an El Niño–Southern Oscillation cold phase event in March–April 1999

Melody A. Avery,[1] David J. Westberg,[2] Henry E. Fuelberg,[3] Reginald E. Newell,[4] Bruce E. Anderson,[1] Stephanie A. Vay,[1] Glen W. Sachse,[1] and Donald R. Blake[5]

Abstract. We examine interhemispheric transport processes that occurred over the central Pacific during the PEM-Tropics B mission (PTB) in March–April 1999 by correlating the observed distribution of chemical tracers with the prevailing and anomalous windfields. The Intertropical Convergence Zone (ITCZ) had a double structure during PTB, and interhemispheric mixing occurred in the equatorial region between ITCZ branches. The anomalously strong tropical easterly surface wind had a large northerly component across the equator in the central Pacific, causing transport of aged, polluted air into the Southern Hemisphere (SH) at altitudes below 4 km. Elevated concentrations of chemical tracers from the Northern Hemisphere (NH) measured south of the equator in the central Pacific during PTB may represent an upper limit because the coincidence of seasonal and cold phase ENSO conditions are optimum for this transport. Stronger and more consistent surface convergence between the northeasterly and southeasterly trade winds in the Southern Hemisphere (SH) resulted in more total convective activity in the SH branch of the ITCZ, at about 6°S. The middle troposphere between 4–7 km was a complex shear zone between prevailing northeasterly winds at low altitudes and southwesterly winds at higher altitudes. Persistent anomalous streamline patterns and the chemical tracer distribution show that during PTB most transport in the central Pacific was from SH to NH across the equator in the upper troposphere. Seasonal differences in source strength caused larger interhemispheric gradients of chemical tracers during PTB than during the complementary PEM-Tropics A mission in September–October 1996.

1. Introduction

The NASA Global Tropospheric Experiment (GTE) sponsored a two aircraft mission (Pacific Exploratory Mission-Tropics B) during March–April 1999 to sample tropospheric air over the tropical Pacific Ocean. Extensive chemical measurements were made from the NASA DC-8 and P-3B aircraft across the Pacific Ocean in both hemispheres. Experimental objectives and aircraft instrumentation during PEM-Tropics B (PTB) are described by *Raper et al.* [this issue]. PEM-Tropics B was designed to complement the earlier PEM-Tropics A (PTA) experiment [*Hoell et al.*, 1999], which occurred during August and September 1996 in the tropical Pacific. Flow patterns over the tropical Pacific during PTA were more representative of climatology than during PTB, which coincided with a more extended and well-developed cold phase El Niño–Southern Oscillation (ENSO) event [*Fuelberg et al.*, this issue].

A major atmospheric circulation feature of the equatorial Pacific is a zonal band of surface convergence between the northern and southern hemispheric low-level easterly trade winds, called the Intertropical Convergence Zone (ITCZ), which is described in detail in the next section. One main scientific objective of PTB was to study the role of the ITCZ as a barrier to interhemispheric transport [*Raper et al.*, this issue]. *Gregory et al.* [1999] examined chemical data from flights across the ITCZ during PTA and discovered that the ITCZ effectively separated northern and southern hemispheric air at altitudes below 5 km. However, there are pronounced seasonal and interannual (ENSO) differences in the wind field and convection patterns in the Pacific equatorial region between PTA and PTB. Seasonal and interannual circulation changes caused some striking altitude-dependent differences in interhemispheric exchange between missions.

This paper combines PTB chemical tracer measurements with meteorological observations to examine the interhemispheric exchange of trace gases, and to present a three-dimensional picture of large-scale transport. We present relevant details of the flow field in the central Pacific during PTB, the distribution of O_3 and the chemical tracers CO_2, CO, and CH_4, and calculate the median concentration of each chemical species. Ozone was measured during PTB by nitric oxide chemiluminesence, CO, and CH_4 by infrared diode laser absorption, and CO_2 by nondispersive infrared absorption. To augment these tracers, we also calculated median concentrations for ethyne (C_2H_2), tetrachloroethylene (C_2Cl_4), methyl iodide (CH_3I), which were measured using gas chromatogra-

[1]Chemistry and Dynamics, NASA Langley Research Center, Hampton, Virginia, USA.
[2]Science Applications International Corporation, Hampton, Virginia, USA.
[3]Department of Meteorology, Florida State University, Tallahassee, Florida, USA.
[4]Department of Earth, Atmospheric, and Planetary Sciences, Massachusetts Institute of Technology, Cambridge, Massachusetts, USA.
[5]Department of Chemistry, University of California, Irvine, California, USA.

phy and mass spectrometry, and for relative humidity, which was measured with a cryogenic hygrometer. These measurement techniques are described in detail by each investigator at: http://wwwgte.larc.nasa.gov/pem/pemtb_meas&model.htm.

Our specific goals are to locate and describe the altitude-dependent dynamical and chemical boundary between the Northern Hemisphere (NH) and the Southern Hemisphere (SH) in this region of the Pacific, and to describe the processes that control the meridional transport of chemical tracers across this boundary. We examine how the double ITCZ structure and the upper tropospheric wind pattern influenced interhemispheric chemical gradients during PTB. We also compare cross-ITCZ chemical gradients during the PTA and PTB missions. The study is limited to the tropical central Pacific, between 25°N to 25°S and 175°E to 140°W, because this region has the most abundant chemical measurements from both hemispheres.

2. Tropical Central Pacific Meteorology During PEM-Tropics B

A general overview of meteorological conditions in the Pacific Basin during PEM-Tropics B is given by *Fuelberg et al.* [this issue]. We focus here on the central tropical Pacific and discuss seasonal and anomalous circulation features that affect the interhemispheric transport of trace gases across the equator. Figure 1 is a plot of mean streamlines at 300, 500, 700, and 1000 hPa over the Pacific, and Figures 2a and 2b are cross sections of the mean zonal and meridional wind components over the tropical central Pacific during the PEM-Tropics B mission. In a general sense, the tropical winds change from easterlies with a strong northerly component at the surface, to westerlies with a strong southerly component in the upper troposphere.

The ITCZ is the dominant circulation feature over the tropical Pacific, which defines a meteorological equator at the boundary of the northeast (NH) and southeast (SH) trade winds. A climatology of the ITCZ in the central Pacific [*Waliser and Gautier*, 1993] shows that the ITCZ has a single structure during most of the year, migrating between 3°-10°N. However, the exact location of the convective region is influenced by the local sea surface temperature distribution [*Barnett et al.*, 1991]. During NH spring (March and April) the ITCZ in the Pacific basin between 160°E and 80°W divides into two zonal bands of convection, one on either side of the equator.

The double ITCZ structure over the Pacific during PTB is evident in images of average rainfall rates for March–April 1999 derived from SSM/I satellite data (Plates 1a and 1b). Convective activity during March–April 1999 appeared to alternate between branches of the ITCZ in the NH and SH [*Hu et al.*, this issue]. However, SSM/I images of average rainfall during March and April suggest that convection in the SH was greater than in the NH during both months. For comparison, Plate 1c shows the SSM/I average rainfall during PTA (September 1996). Tropical rainfall associated with the ITCZ in the NH is greater during PTA than during PTB (indicating more convection) but confined to a narrow zonal band between 5°N and 10°N, more like the idealized view of the ITCZ as one solid band of convection.

Although typical of March and April, the double ITCZ was enhanced by cold ENSO event flow anomalies during PTB, particularly the strength of convection in the SH branch. The double ITCZ structure over the central Pacific results from a
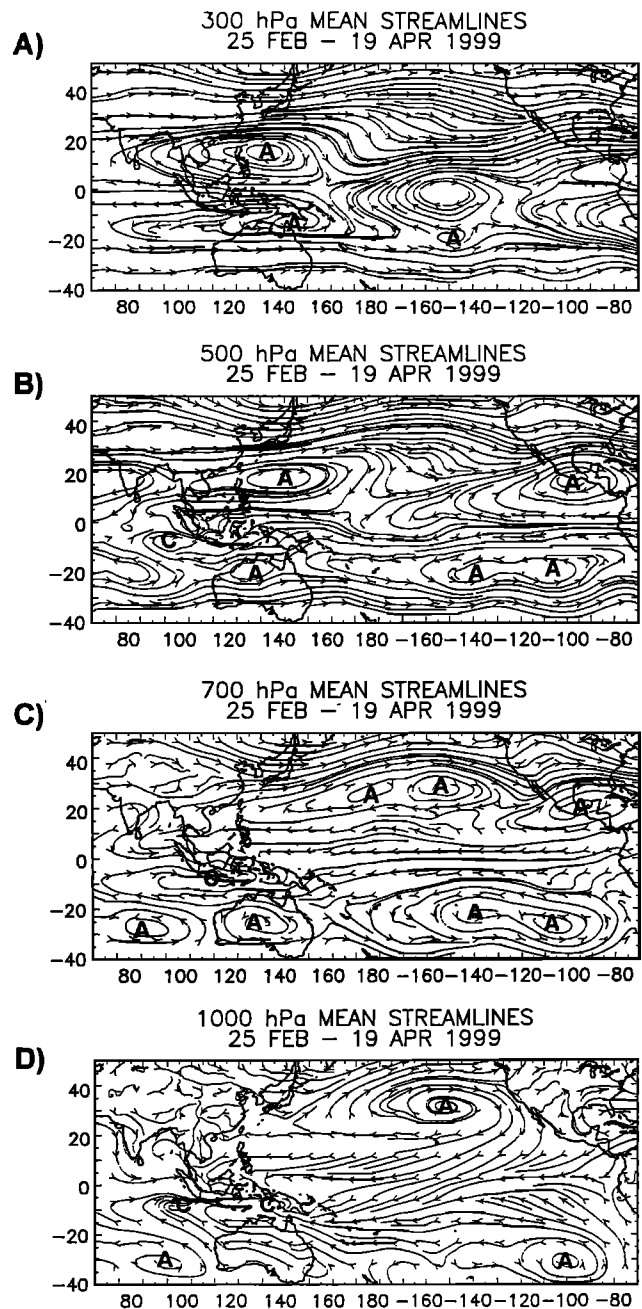

Figure 1. Mean streamlines on constant pressure surfaces during PEM-Tropics B, calculated from ECMWF analysis data at Florida State University. This figure shows streamlines at (a) 300 hPa, (b) 500 hPa, (c) 700 hPa, and (d) 1000 hPa. Anticyclonic circulation centers are labeled as "A," and cyclonic circulations are labeled with "C."

relaxing of the southeast trade winds, which are affected by both seasonal and interannual variations in the location of the South Pacific anticyclone and sea surface temperatures [*Waliser and Gautier*, 1993]. Although there is much cross-equatorial symmetry, Figure 1d shows that the South Pacific high-pressure center is located significantly farther east (40°S, 95°W) than the center of the NH anticyclone (35°N, 150°W). During PTB, colder sea surface temperatures combined with the anomalous southeastern location of the South Pacific anticyclone caused convergence of the northeasterly and south-
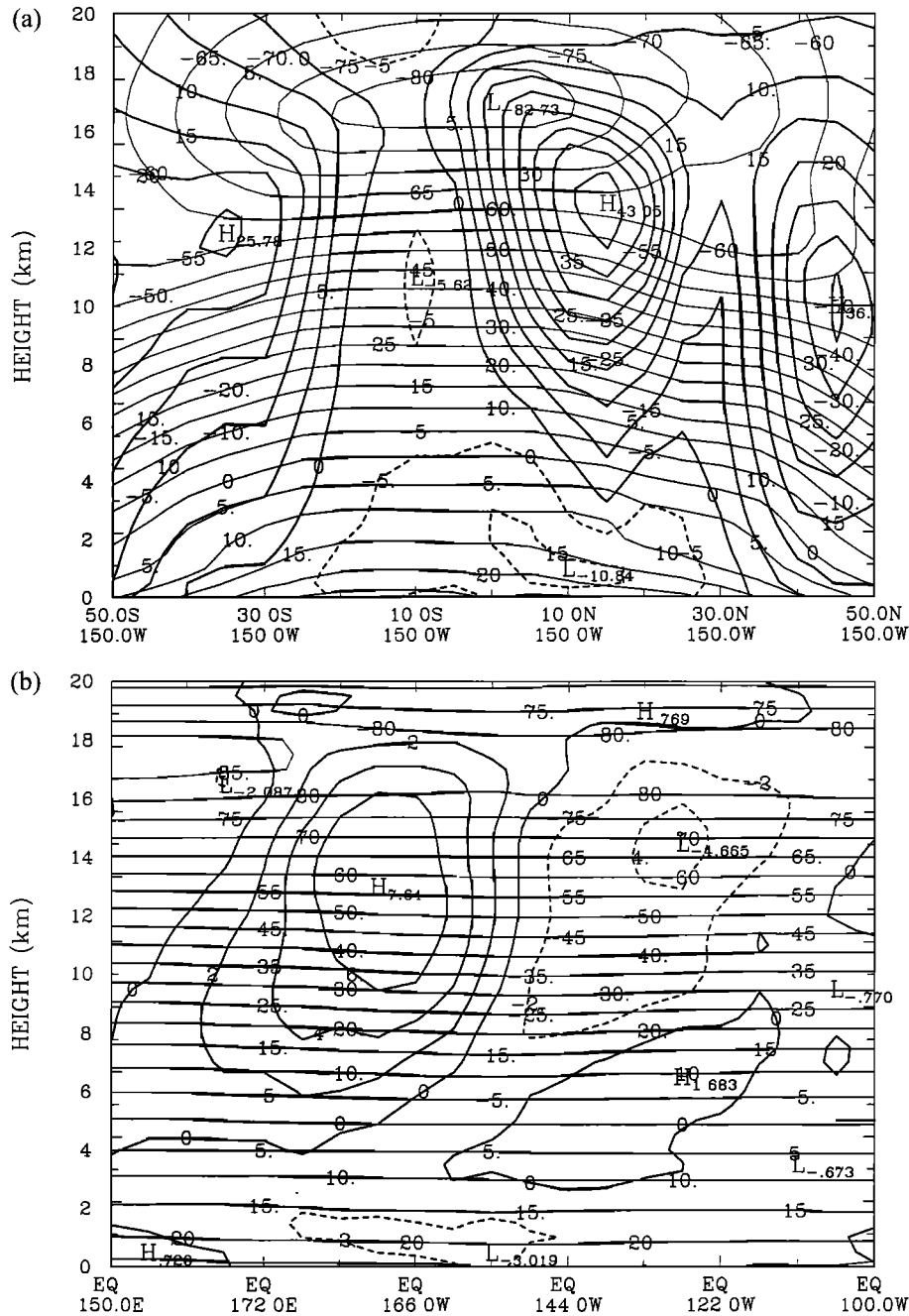
Figure 2. Mean zonal and meridional wind cross sections drawn by Yong Zhu at the Massachusetts Institute of Technology from 51-level ECMWF data obtained through Meteo France for the PEM-Tropics B period (March 1 to April 19, 1999). (a) Mean zonal wind at 150°W. Solid contour lines represent westerly winds, while dashed contours represent easterly winds. (b) Mean meridional winds at the equator. Solid contours represent southerly winds, while the dashed contours are northerly.

easterly surface equatorial trade winds to occur in the SH instead of the NH over the central Pacific. Plate 2 is a time series of wind vectors measured by instruments on the NOAA Tropical Atmospheric Ocean (TAO) array of buoys at 170°W. There is a shift in wind direction, with a significant increase in the northerly component of the winds between 0°–5°N, which develops in February and continues through March and April. Weakened convergence in this region was insufficient to generate the lifting and resulting convection that ordinarily forms the northern branch of the ITCZ. In the SH at 5°–8°S, in-

creased convergence in the surface winds appears at the beginning of March, coincident with the appearance of the ITCZ in the SH.

Plate 3 shows a time series of the 5-day mean meridional component of the TAO buoy winds averaged between 2°N–2°S. The meridional wind component is northerly between 170°E and 140°W, with maximum wind speeds occurring during February, March, and April. The meridional wind anomaly, also shown in Plate 3, shows that east of 175°E, near the equator, the deviation from climatology is northerly through-
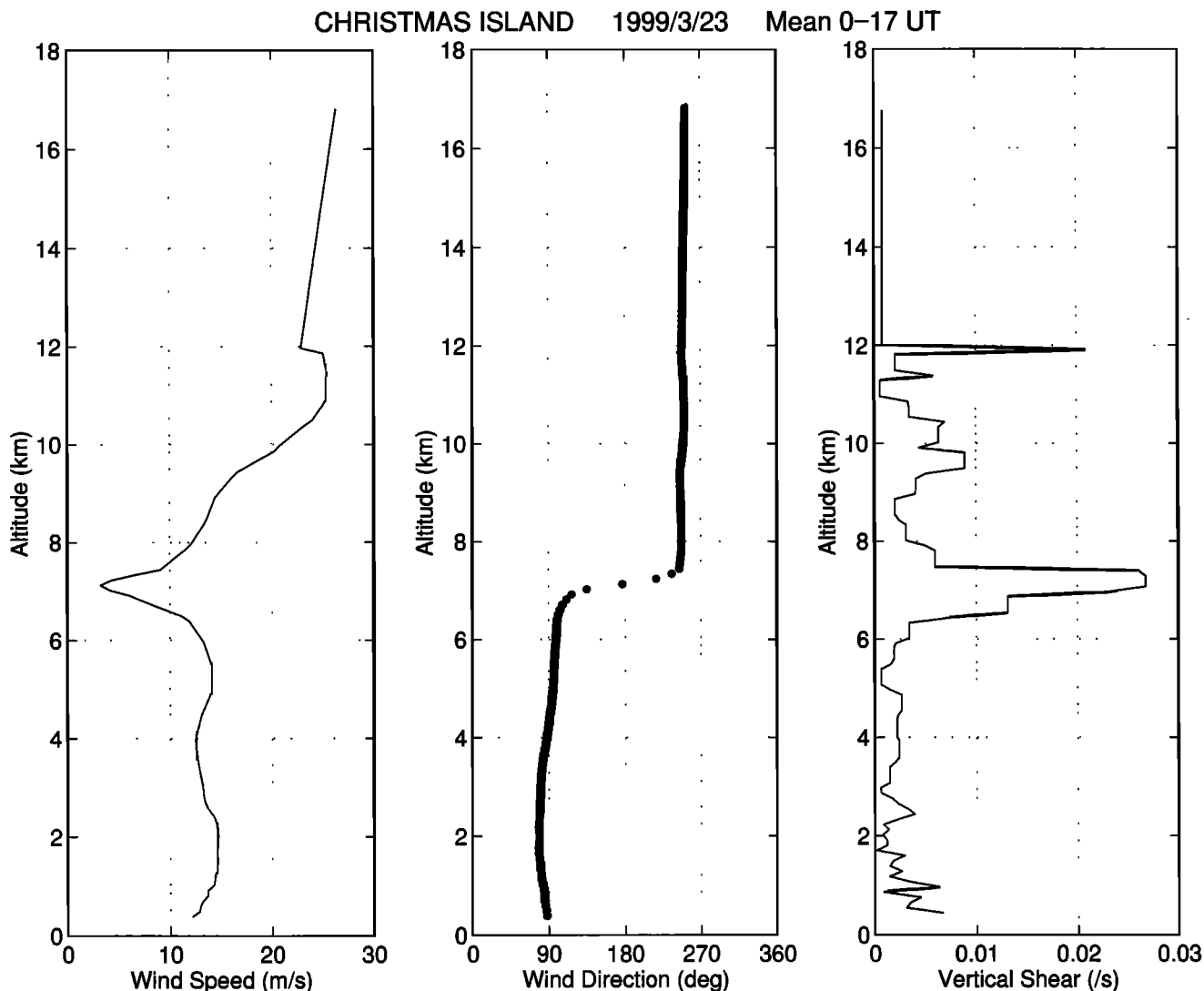
Figure 3. Mean 0000–1700 UT wind speed, direction, and vertical shear profiles measured at 2°N, 156°W on March 23, 1999. The measurements were made using the NOAA Aeronomy Laboratory radar system located at Christmas Island.

out this time period. The anomaly is 1–3 m s^{-1}, compared to mean wind speeds of 2–4 m s^{-1}. Although these speeds are light, they suggest that transport across the equator due to the cold phase of ENSO is as large as climatology during March and April.

Altitudes between 4–7 km represent a transition region where tropical wind speeds are light and flow patterns are complex. Figure 3 shows the vertical wind shear measured during PTB with a wind profiler located at Christmas Island (2°N, 157°W). The wind profile on this day shows the change in wind speed and direction, with maximum vertical wind shear at 7 km (between 400 and 500 hPa). Mean streamlines on the 500 hPa pressure level are illustrated in Figure 1b. There is a col at 175°E, 5°N, a trough southwest of Hawaii at 10°N, and an anticyclonic circulation at 100°W, 5°S, just off the southern Mexican coast. Air from the SH and equatorial region flows around the west side of this anticyclone into the NH between 140°W and 175°E. Between 10°–15°N this flow converges with the midlatitude NH westerlies, combining air originating from both hemispheres.

A common interannual variation in upper level jet structure

that is correlated to the ENSO cycle is the appearance of a double jet in the NH during ENSO cold events [*Kiladis and Mo*, 1998]. The double jet structure is evident in the 300 hPa mean streamlines during PTB, Figure 1a. During PTB the flow above 7 km in the NH is dominated by the anomalous southern branch of the NH jet (Figures 1a and 2a). The meridional upper level flow is southerly, across the equator west of 160°W due to a strong and persistent upper level clockwise divergent circulation at the equator, centered at 150°W. This flow is anomalous and joins the southern NH jet. The return flow is northerly above 8 km and east of 140°W. Most PEM-Tropics B sampling was performed on the west, or southerly side of the circulation, so most large-scale transport of chemical tracers across the equator observed during the mission in the upper troposphere was from the SH into the NH.

3. Cross-ITCZ Comparison: Methodology

Measured chemical tracer concentrations during each PTB flight were sorted into three regions, corresponding to the
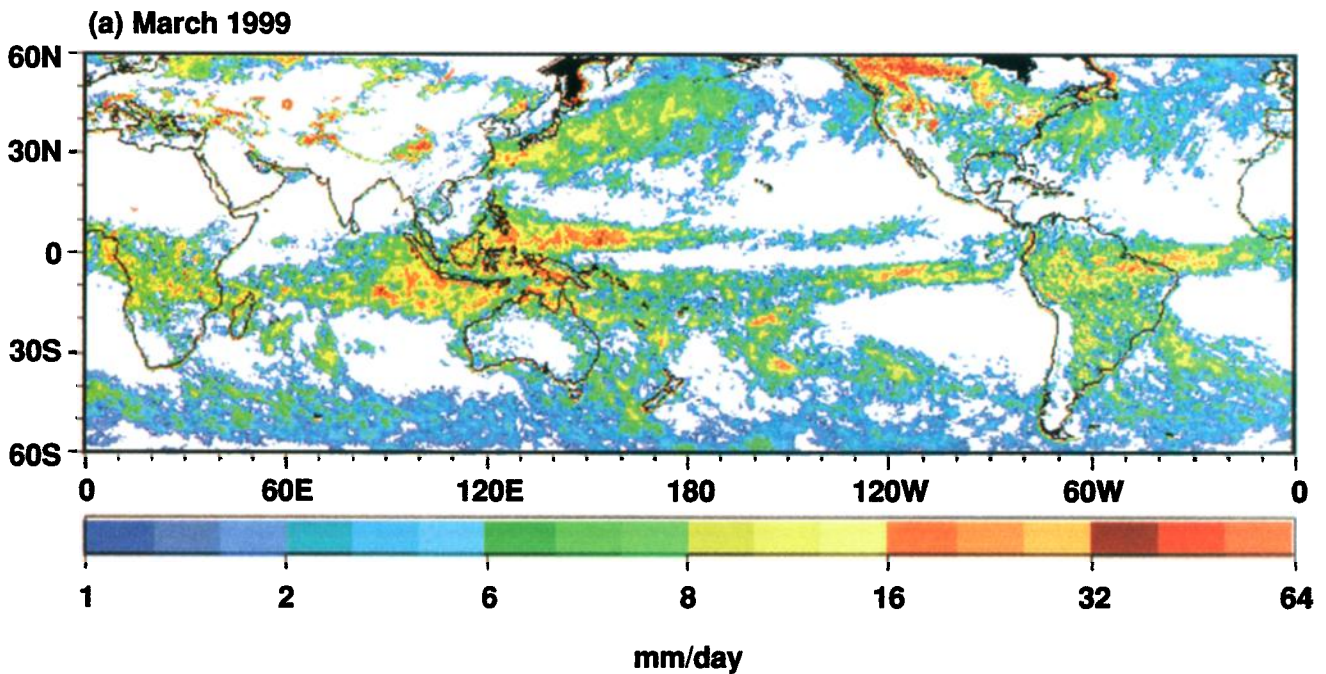
(a) March 1999

Plate 1. Global rainfall rates derived using the Ferriday algorithm on SSM/I satellite data. Average rainfall rates during (a) March and (b) April 1999 (during PEM-Tropics B); (c) average rainfall rate during September 1996 (during PEM-Tropics A). Note the double structure of the ITCZ during April 1999, and the narrower spatial distribution of rainfall in the tropics at the ITCZ and SPCZ during PEM-Tropics A. These images were downloaded from the NOAA Environmental Technology Laboratory climate image archive at URL: http://www1.etl.noaa.gov/climsat/archive.html.

division of the tropical central Pacific by the northern and southern branches of the ITCZ. These regions are north of the ITCZ in the northern hemisphere, south of the ITCZ in the southern hemisphere, and the equatorial region between branches of the ITCZ.

Data from flights within the central Pacific study region of 175°E to 140°W and 25°N to 25°S were included if they crossed at least one branch of the ITCZ. Flights were not included when sampling was concentrated at a particular location or altitude. The 10 appropriate flights identified for this analysis are listed in Table 1, and the spatial coverage of these flights within the study region is illustrated in Plate 4. The range of altitudes sampled was evenly distributed in both hemispheres. However, measurements in the NH have a smaller longitudinal range because NH tropical sampling was limited to flights south of Hawaii. Although the *Gregory et al.* [1999] study of PTA only used data from the DC-8, we have included in situ data from the P-3B because P-3B samples expand and balance

the latitude and altitude distribution of the measurements at pressures above 400 hPa.

We identified the location of an ITCZ branch along each flight track by looking for the latitude of greatest convergence in the surface winds that was associated with convection. First, we found locations of convergence in the near-surface wind field, calculated from high-resolution ECMWF assimilated data. Because the assimilated data is highly uncertain in the tropics, we used the TAO buoy winds (Plate 2) to verify the latitude of maximum surface convergence. We also examined GOES 10 satellite images to locate active convective clouds that were associated with the ITCZ.

The average latitude of the ITCZ in the NH was 6.8°N, with less than 1° variance among the flights sampled. During several flights there was only weak convergence along the ITCZ in the NH, so we divided the data based on the latitude of greatest change in the meridional wind speed as measured on the TAO buoys. The average location of the southern ITCZ branch was

Table 1. PEM-Tropics B Flights Analyzed

Plane	Flight	Day	Date	Region
P-3B	5	72–73	March 13–14, 1999	ITCZ north; 0°–20°N, 155°–158°W
DC-8	7	72–73	March 13–14, 1999	ITCZ north; 1°S–20°N, 154°–165°W
DC-8	8	74–75	March 15–16, 1999	ITCZ north; 0°–19°N, 152°–158°W
DC-8	9	76–77	March 17–18, 1999	ITCZ north and south; 19°S–19°N, 155°–182°W
P-3B	9	79	March 20, 1999	equatorial; 0°–3°N, 140°–158°W
P-3B	12	85–86	March 26–27, 1999	ITCZ south; 3°N–18°S, 149°–166°W
DC-8	13	85–86	March 26–27, 1999	ITCZ south; 22°–3°S, 182°–149°W
P-3B	13	90–91	March 31 to April 1, 1999	ITCZ south; 18°–6°S, 142°–150°W
DC-8	17	97	April 7, 1999	ITCZ south; 18°–0°S, 142°–150°W
P-3B	17	99–100	April 9–10, 1999	ITCZ north and south; 19°S–21°N, 149°–158°W

(b) April 1999

Plate 1b. (continued)

(c) September 1996

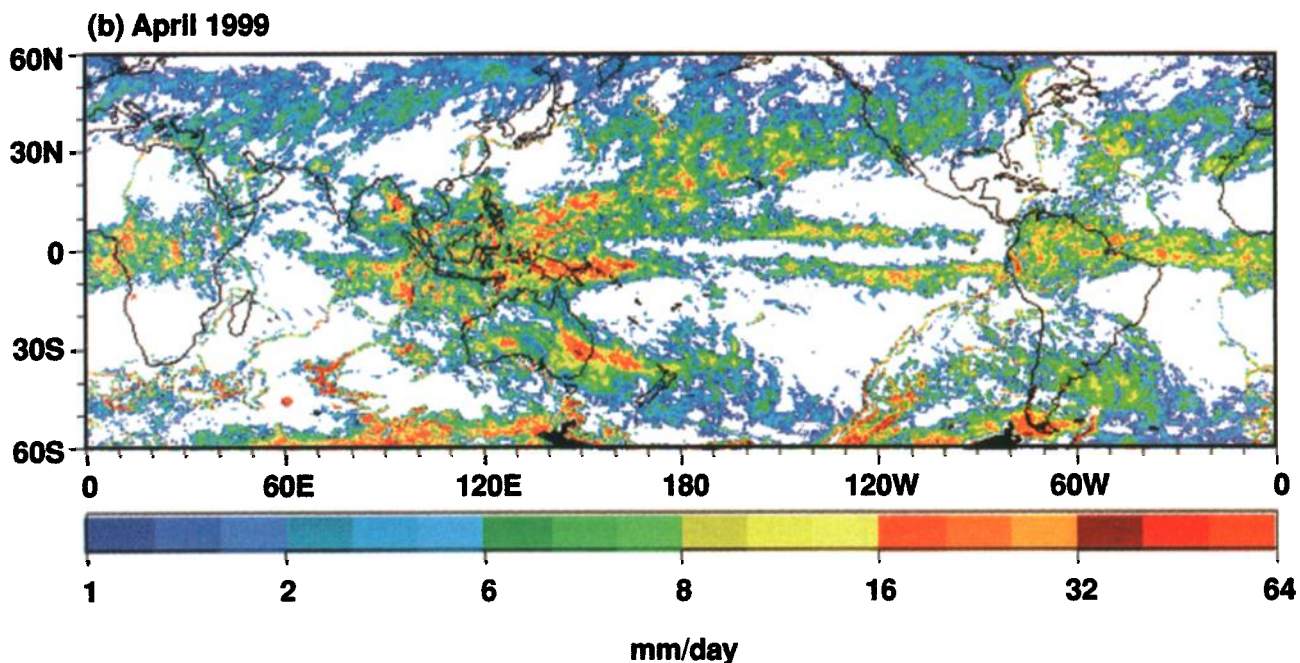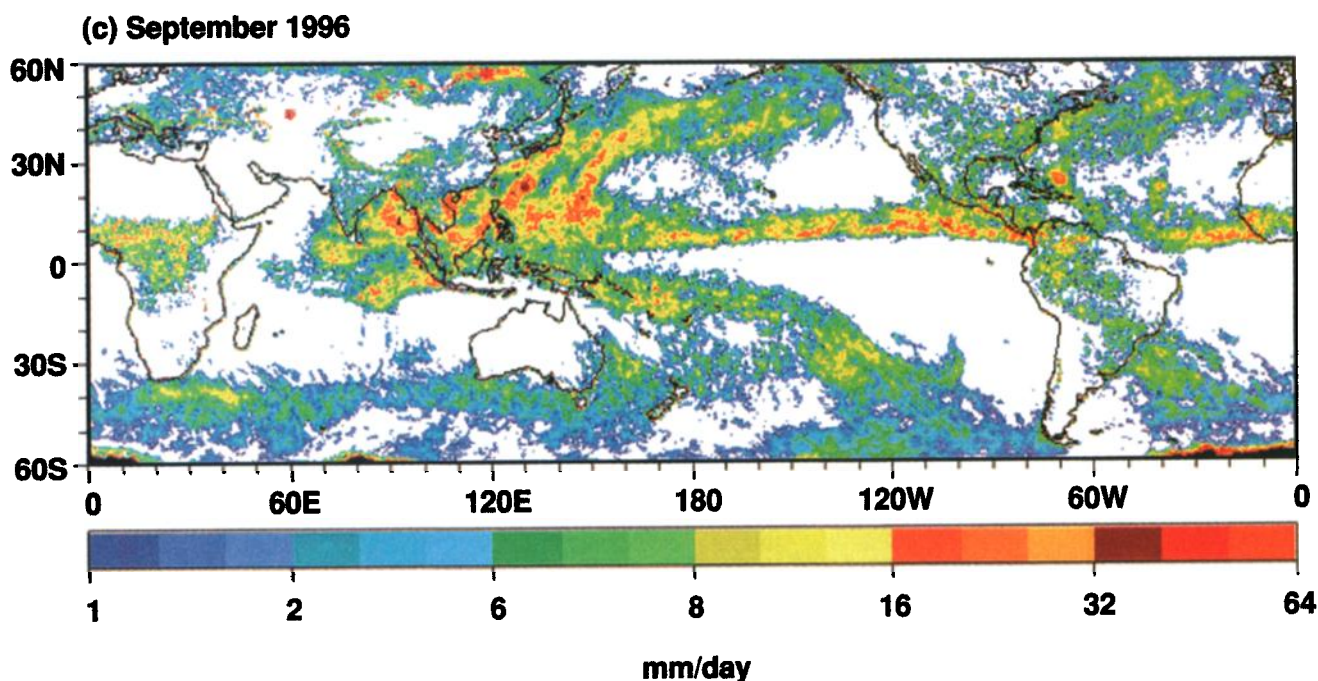**Plate 1c.** (continued)

5.8°S, with a larger variance of 1.6°. Division of the upper level data was somewhat arbitrary since the ITCZ is only potentially effective as a barrier to transport at low altitudes where the winds are convergent. For simplicity and consistency, we have chosen to divide the high-altitude data at the same latitude as the near-surface data. Chemical data within ±1° latitude of each branch of the ITCZ were not included in our calculations of median chemical concentrations to allow for error in the precise location of the boundaries.

The chemical measurements were sorted into bins at six different vertical levels. The vertical bins represent pressures greater than 900 hPa, 800–900 hPa, 600–800 hPa, 400–600 hPa, 300–400 hPa, and less than 300 hPa. These pressures correspond to altitudes of approximately 0–1 km, 1–2 km, 2–4 km, 4–7 km, 7–9 km, and 9–12 km, respectively. The first vertical bin represents the surface and near-surface boundary layer, the 1–2 km bin includes the mandatory 850 hPa pressure level, 2–4 km includes the 700 hPa level, and 4–7 km includes the 500 hPa level and represents the transition layer between the upper and lower troposphere.
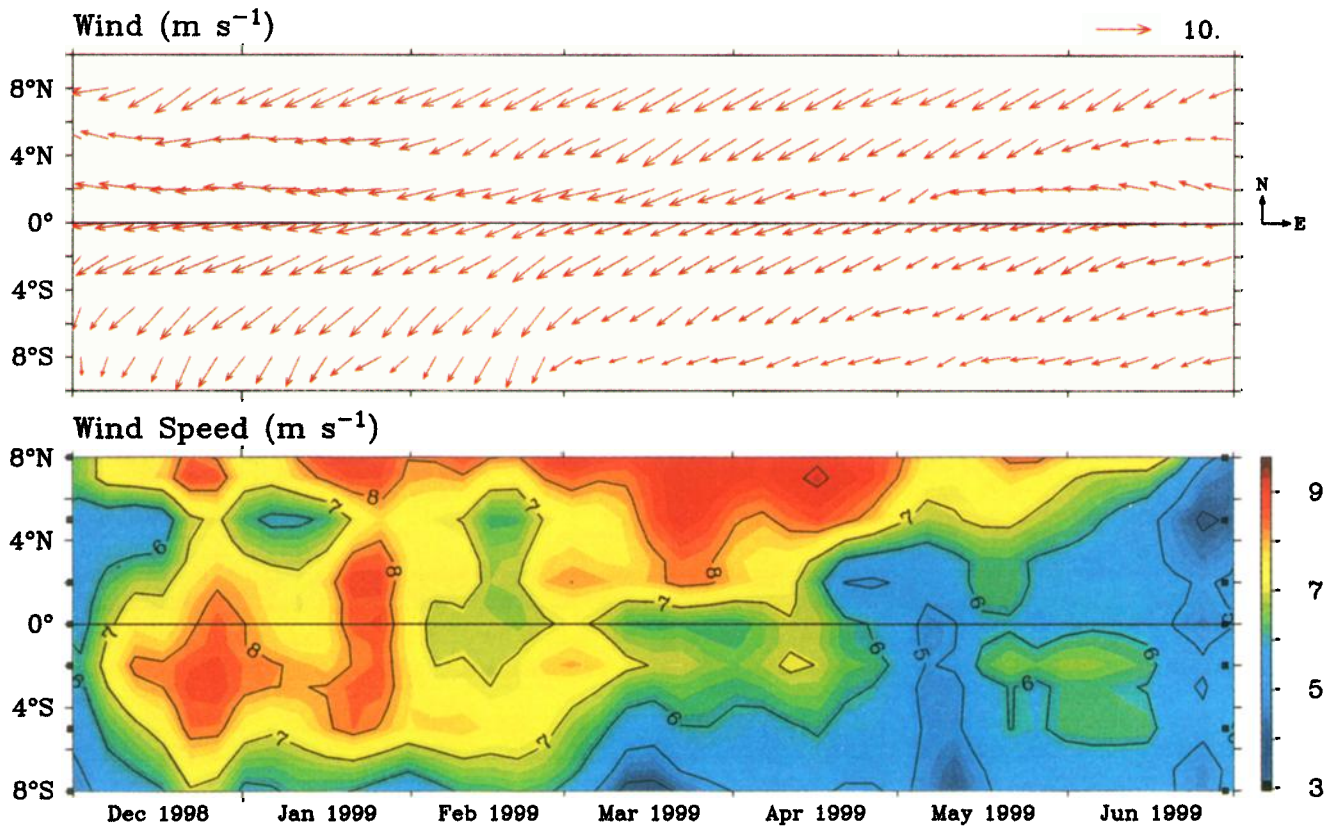
Plate 2. Time series of (top) 5-day mean wind vectors and (bottom) wind speed at 170°W measured by instruments on the NOAA PMEL Tropical Atmosphere Ocean (TAO) array of buoys from December 1998 through June 1999. Plots of the buoy data were provided by the TAO project office website at http://www.pmel.noaa.gov/toga-tao. In the NH the time series of winds measured at 0°, 2°, and 5°N shows that the northerly component of the easterly trades developed from February through April 1999. Convergence between the NH and SH trade winds at the surface during that time is missing in the NH. This coincides with observations indicating greatly reduced convective activity at the NH branch of the ITCZ.

Median concentrations of trace gases in the highest two altitude bins were calculated only from DC-8 measurements because the P-3B did not fly at pressures lower than 400 hPa. Air sampled in these highest altitude bins exhibits a significant stratospheric influence [Browell et al., this issue]. We have not filtered out stratospherically influenced air from our data set because we do not want to eliminate this contribution to the bulk composition of the troposphere during the PTB mission. Using a similar philosophy, we have not attempted to filter out plumes of air containing greater than average amounts of combustion-related tracers. DC-8 samples in clouds not associated with active convection did not reveal significant differences between chemical tracer concentrations in cloudy and clear air (M. Avery and R. Russo, unpublished study, 2000). Therefore we have included chemical data from both cloudy and clear air sampling, except when the planes were flying through active convective cells, which occur at the ITCZ branches and form the boundaries of the study region.

4. Chemical Tracer Results

The large-scale transport patterns discussed in the previous section are reflected in latitudinal chemical tracer distributions. We focus here on carbon dioxide (CO_2), methane (CH_4), and carbon monoxide (CO). The first two species have extended photochemical lifetimes of 4–7 years, and ~10 years,

respectively. The photochemical lifetime of CO is significantly shorter, about 6 weeks in the marine tropics (J. Crawford, personal communication, 2000). Ozone (O_3) also provides valuable information about transport patterns even though it is not a conserved chemical tracer.

CH_4, CO, and CO_2 are emitted by the combustion of fossil fuels during anthropogenic activities, and from natural and anthropogenic biomass burning. CH_4 is emitted by microbial processes in anaerobic environments, both natural and related to agriculture. CO is a precursor to ozone formation and can also be formed by CH_4 oxidation. The NH has a larger landmass than the SH, with more biological activity and a larger population causing greater anthropogenic fossil fuel consumption. This causes mean concentrations of CO and CH_4 to be significantly greater in the NH than in the SH. CO_2 has a pronounced seasonal cycle [Vay et al., 1999] because of a wide variety of biological sources and sinks, most notably photosynthesis. During PTB, CO_2 concentrations were greater in the NH than the SH because photosynthesis rates were reduced during the NH winter and because there was an increase in the combustion of fossil fuels used during the NH winter for heating.

Plates 5a–5d are latitudinal cross sections of O_3, CO_2, CO, and CH_4 from the composite of all PTB flights within the central Pacific study domain (175°E–140°W, Plate 4). The long-lived tracers CO_2 and CH_4 have similar vertical and lat-
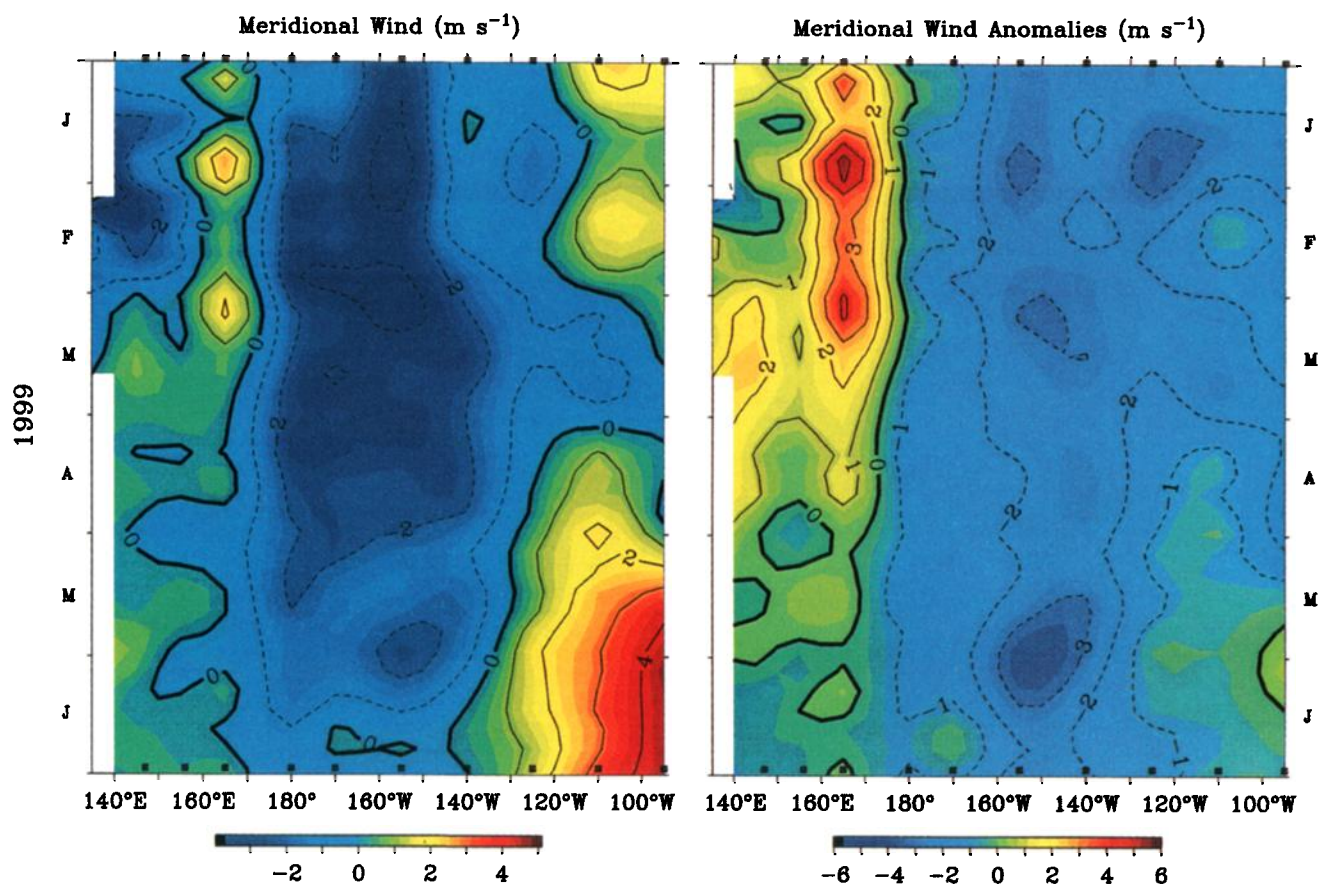
Plate 3. Longitudinal time section of the mean meridional TAO buoy wind component averaged between 2°N and 2°S. The time section runs from January (at the top) through June 1999. Southerly winds are contoured in yellow, orange, and red, while northerly winds are shades of green and blue. The anomalous wind is calculated by subtracting the Comprehensive Ocean Atmosphere Data Set (COADS) wind climatology from the measured buoy winds. During January–June 1999 the equatorial winds between 170°E and 140°W are northerly, as is the anomaly. These plots were provided by the TAO project office.

itudinal distributions, and generally exhibit greater concentrations in the NH. The same pattern is evident in the CO distribution, despite its much shorter photochemical lifetime.

The region of the sharpest horizontal gradient between surface NH and SH concentrations of CO_2 and CH_4 (5°–10°S) includes the average location (~6°S) of the SH branch of the ITCZ, indicating that the low-altitude chemical and dynamical interhemispheric boundary was most often in the SH during PTB. This is consistent with mean streamline patterns (Figure 1d) and our discussion in section 2, which shows this is the location of greatest convergence between the NH and SH trade winds.

Figures 4 and 5 show vertical profiles of median O_3, CO_2, CO, CH_4, C_2H_2, C_2Cl_4, CH_3I, and ultrafine particles for the three regions of the central Pacific during PTB. These results generally reinforce the chemical tracer distribution shown in Plate 5, with median concentrations of CO_2, CO, and CH_4 below 4 km in the equatorial region between ITCZ branches intermediate to SH and NH values because of transport and mixing of NH air into the SH. Above 4 km, medians of these species in the equatorial region are closer to cleaner SH values.

The transition region of the NH between 4–8 km exhibits streamline (Figure 1b) and chemical tracer patterns (Plate 5) that are more complicated than those in the upper or lower troposphere. However, CH_4, CO_2, and CO concentrations in the equatorial region are similar to SH values, suggesting net

SH to NH transport across the equator in the middle troposphere during PTB. The sharp horizontal gradient of these tracer concentrations in the middle troposphere near 10°–15°N results from convergence between the subtropical NH westerlies and circulation of SH air around the western side of the midlevel anticyclone in the eastern Pacific at 100°W, as discussed in section 2.

Low-altitude median O_3 profiles for NH, SH, and equatorial regions (Figure 4a) show the interhemispheric O_3 gradient is much different than that of the relatively long-lived chemical tracers CO, CO_2, and CH_4. Median concentrations of CO, CH_4, and CO_2 below 4 km in the equatorial region are similar to NH values due to transport across the equator by the northeasterly trade winds. In contrast, near-surface equatorial O_3 is lower in the equatorial region than it is in the SH. The reason for this is that O_3 is destroyed efficiently near the surface in the tropics by sunlight and water vapor as it is transported. *Olson et al.* [this issue] have documented substantial O_3 loss below 4 km in the tropics, and estimate the diurnal average photochemical lifetime of O_3 as only about 5–6 days (J. Olson, personal communication, 2000). The lowest ozone concentration measured during PTB was at the surface near Fiji (175°E), at the western boundary of the northeasterly trade winds.

At high altitudes in the equatorial NH, high O_3 concentrations (Plate 5a) coincide with the location of the anomalous
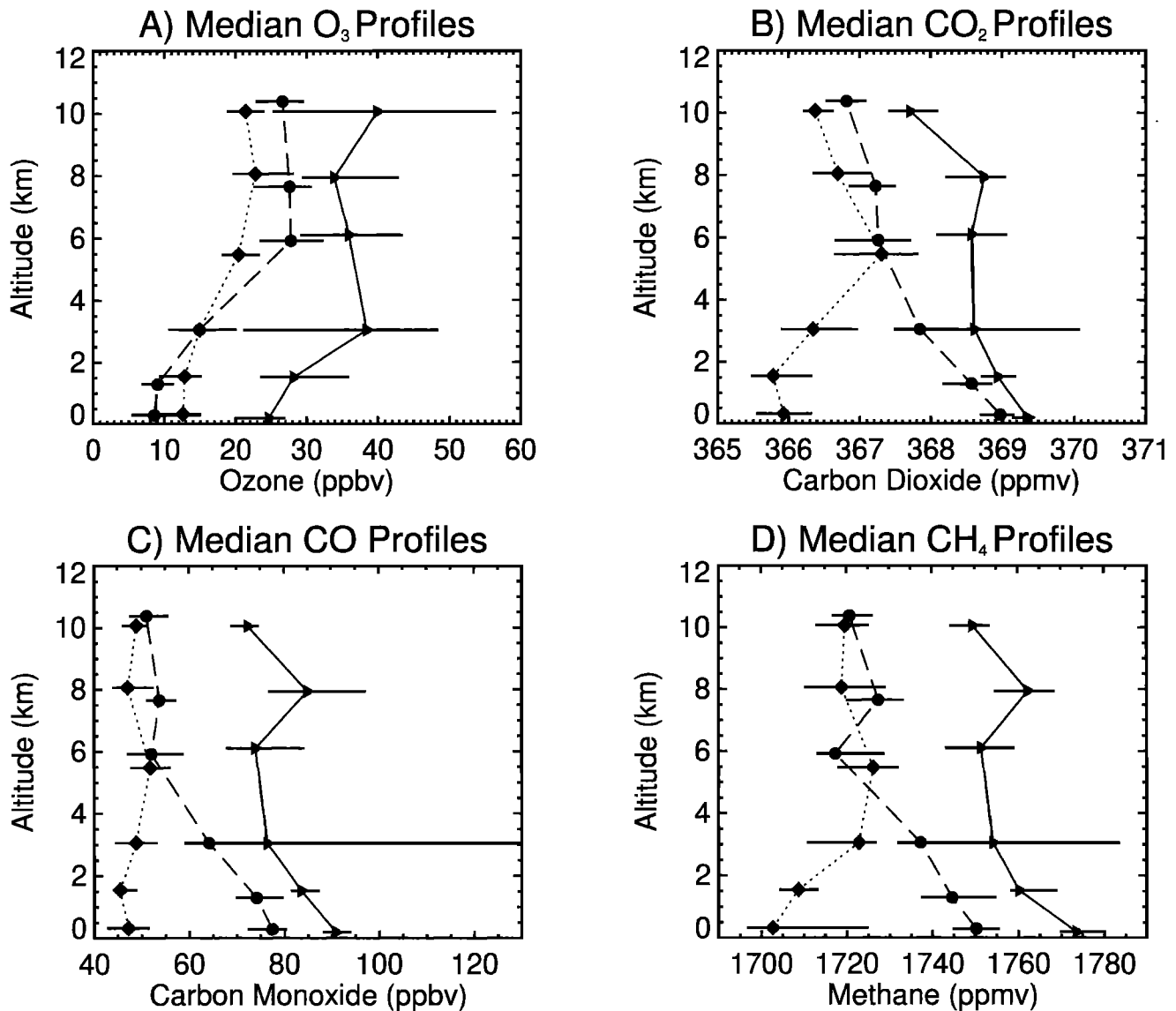
Figure 4. Median profiles of (a) ozone, (b) carbon dioxide, (c) carbon monoxide, and (d) methane in the central Pacific. Northern hemispheric values are plotted as triangles, medians from the equatorial region are plotted as circles, and those from the SH are plotted as diamonds. Sidebars on the median values denote the first and third quartiles. The profiles are connected for clarity.

southern branch of the Pacific subtropical jet discussed in section 2, and with enhanced potential vorticity (ECMWF analysis) typical of the lower stratosphere. We observed this stratospheric contribution to the equatorial and subtropical NH upper troposphere where there is also jet-related meridional shear and eddy momentum flux [Shapiro et al., 2000]. This mechanism is only likely to be significant at latitudes less than 25°N when the Pacific subtropical jet bifurcates during cold ENSO events. Elevated O_3 concentrations at 9–12 km in the SH (25°–30°S, Plate 5) were observed in the subtropical SH while crossing extratropical frontal boundaries, as opposed to being directly associated with an anomalous jet.

CO_2, CH_4, and CO all appear to be well mixed vertically in the SH, consistent with the large amount of SH convection observed in the meteorological data, and with more distant surface sources. Surface concentrations of CH_4 are 1740–1785 ppbv in the NH tropics and 1695–1725 ppbv in the SH tropics.

CO concentrations are less than 60 ppbv in the SH tropics, and greater than 75 ppbv in the NH tropics near the surface. Cross-equatorial flow in the upper troposphere (Figure 1a, 140°–180°W) transported low SH concentrations of CO (<60 ppbv) and CH_4 (<1725 ppbv) into the NH at high altitudes, visible in Plate 5. CO_2 distribution in the upper troposphere also shows the same pattern, including sinking motion observed in the ECMWF vertical winds from 0°–5°N, in the equatorial region between ITCZ branches. The mean vertical velocity in the equatorial region was downward between ascending air at the SH and NH ITCZ branches [Fuelberg et al., this issue].

5. PEM-Tropics Missions A and B Cross-ITCZ Comparison

Figures 6 and 7 compare median tracer concentrations north and south of the ITCZ during PTA [Gregory et al., 1999] with
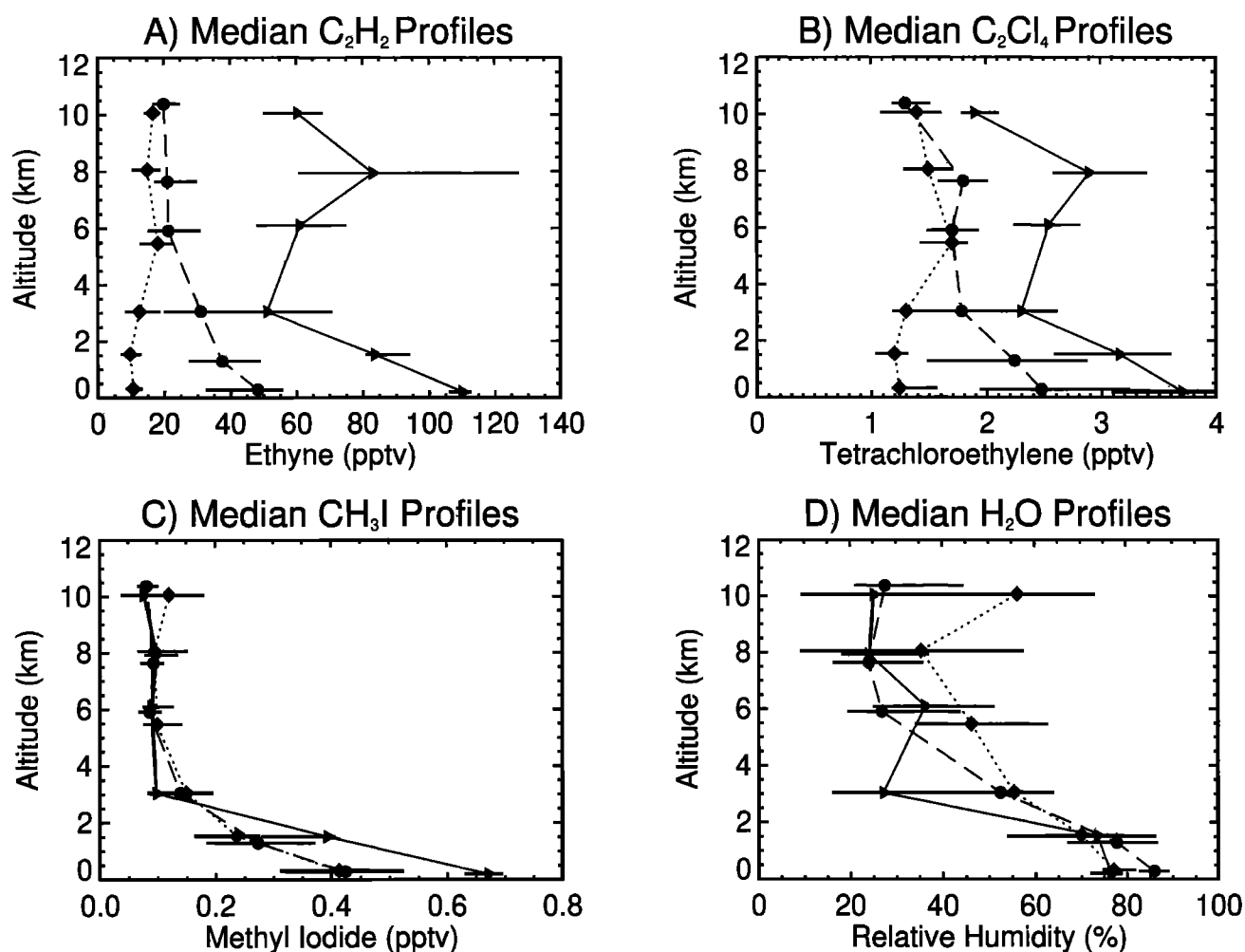
Figure 5. As in Figure 4, except that median profiles for (a) ethyne, (b) tetrachloroethylene, (c) methyl iodide, and (d) relative humidity are shown.

our results from PTB. Below 4 km, median O_3 concentrations in the NH are greater during PTB than during PTA. In the middle tropospheric SH, O_3 concentrations are much larger during PTA. The influence of biomass burning in the SH during PTA contrasts with greater vertical convective mixing in the SH during PTB. At high altitudes (above 8 km) in the NH tropics, median O_3 values of 30–35 ppbv measured during both missions may represent a tropical upper tropospheric background concentration, due to rapid global long-range transport.

Figure 6b illustrates median CO_2 concentrations from PTA and PTB. The surface concentration of CO_2 during PTB in the SH tropics is 365–367 parts per million by volume (ppmv), compared with 360–362 ppmv during PTA [*Vay et al.*, 1999]. In the NH tropics, surface CO2 concentrations range between values of 368–371 ppmv, with a large subtropical CO_2 source indicated by the surface maximum between 25°–30°N (Plate 5). In contrast, surface concentrations of CO_2 measured during PTA in the NH north of the ITCZ range between 359–360 ppmv.

These differences between missions reflect a secular, temporal increase in CO_2 concentrations, and the seasonal difference in mission timing. The direction of the interhemispheric gradient was reversed between PTA and PTB, with greater

CO_2 in the NH during PTB. PTA occurred in the NH autumn at the minimum of the CO_2 seasonal cycle, while PTB occurred near the peak of the NH CO_2 cycle. Concentrations of CO_2 are greater in the SH during PTA because of biospheric uptake of CO_2 during the NH summer. This produced a cross-hemispheric gradient of 1 ppmv. During PTB the seasons and the CO_2 gradient were reversed, and a larger CO_2 gradient of 3–4 ppmv was observed between the NH and SH.

Median concentrations of CO_2 and CH_4 were greater in both hemispheres during PTB than during PTA. The difference between average (NH and SH) surface concentrations of CO_2 and CH_4 in the 30 months between missions is 6.5 ppmv and 27 ppbv, respectively, compared to the global average seasonal fluctuation of about 1 ppmv in CO_2, and 15–17 ppbv in CH_4. This change in temporal concentration appears consistent with globally averaged growth rates of 1–3 ppmv/year for CO_2, and 3–15 ppbv/year for CH_4, measured by the NOAA Climate Monitoring and Diagnostics Laboratory cooperative sampling network (http://www.cmdl.noaa.gov/ccgg). The maximum growth rates correlate with the climatologically significant ENSO warm event that occurred during 1998 between missions. CH_4 mixing ratios at all altitudes in both hemispheres are greater during PTB, indicating that the global trend was
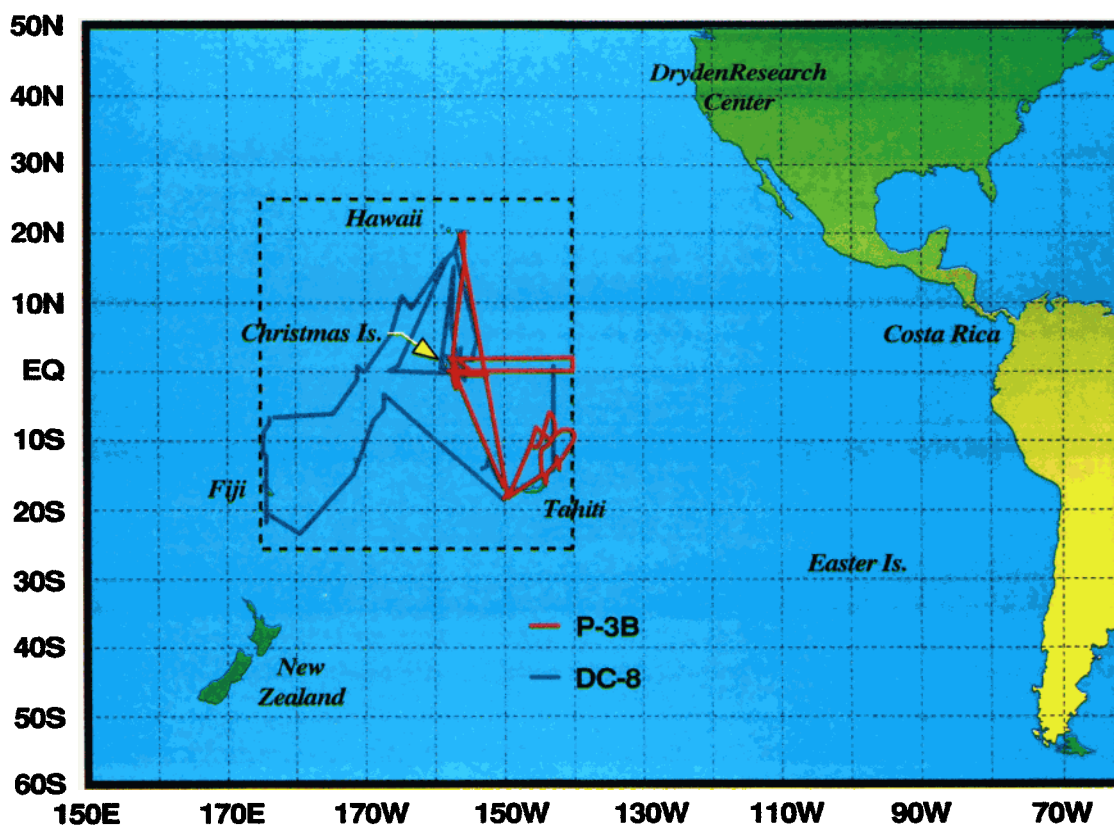
Plate 4. Flight tracks of the DC-8 (blue) and the P-3B (red) over the central Pacific, where data were used to calculate median chemical concentrations. The yellow arrow on the plate shows the location of Christmas Island, at 157°W. The longitudinal distribution of measurements is smaller in the NH than in the SH.

larger than the seasonal biomass burning influence observed during PTA.

The direction of upper-level transport also reversed between PTA and PTB. Large-scale transport of CO_2-depleted air from the NH into the SH occurred in the upper troposphere during PTA [*Vay et al.*, 1999], while (Plate 5) during PTB air containing less than 367 ppmv was advected from the SH across the equator into the NH at altitudes above 8 km. SH CO_2-depleted air also was measured on the northern side of the equator in the middle troposphere during PTB and correlates with the region of descending air near the equator between ITCZ branches. Above 8 km the interhemispheric gradient in CH_4 disappears, consistent with the advection of CH_4-poor SH air into the NH at high altitudes. C_2H_2 is a hydrocarbon emitted by the incomplete combustion of fossil fuels or by biomass burning [*Blake et al.*, this issue]. *Bergamaschi et al.* [2001] found a very high correlation between CO and C_2H_2 in the central Pacific from shipboard measurements made during 1996–1998, and we also find that they were highly correlated during PTB. With similar photochemical lifetimes of about 6 weeks in the tropical Pacific, it is useful to compare CO and C_2H_2 distributions with longer-lived tracers CO_2 and CH_4. Figure 5a is a plot of the median profiles of C_2H_2 during PTB, and Figure 4c is a plot of CO profiles. Equatorial and SH concentrations of both species are similar above 4 km. At altitudes below 4 km, equatorial median CO and C_2H_2 concentrations are intermediate between equatorial NH and SH values. They are fractionally closer to SH concentrations than CO_2 and CH_4, due to more rapid chemical destruction during transport. Figures 6c and 7a

compare median PTA and PTB CO and C_2H_2 profiles. Both CO and C_2H_2 are greater at all altitudes in the SH during PTA than during PTB, reflecting a greater influence from biomass burning. In the NH, CO and C_2H_2 concentrations are greater during PTB, coinciding with larger O_3 concentrations and the upper tropospheric transport of polluted air from Asia and Europe [*Maloney et al.*, this issue].

C_2Cl_4 is an industrial solvent with a chemical lifetime of 1–4 months. It is a useful tracer for NH urban or industrial emissions not related to fossil fuel combustion [*Blake et al.*, 1999]. Figure 5b is a plot of median C_2Cl_4 profiles from PTB, and Figure 7b compares medians from PTB with those from PTA. C_2Cl_4 concentrations are 0.1–0.15 pptv greater in the NH during PTB at all altitudes because of greater urban influence on the NH tropical Pacific. In the SH, C_2Cl_4 concentrations are as much as 0.4 pptv greater during PTB than during PTA, due to increased low-altitude transport of NH air into the SH. This contrasts with observations of elevated CO and C_2H_2 correlated with low C_2Cl_4 in the SH during PTA, since biomass burning does not emit C_2Cl_4.

CH_3I has a biological, oceanic surface source, and is useful with enhanced relative humidity as an indicator of vertical convective mixing above the marine boundary layer [*Cohan et al.*, 1999]. CH_3I is not very soluble and has a lifetime of about 4 days. Figure 5c is the PTB profile of median CH_3I, and Plate 7c is the PTA/PTB comparison. Concentrations of CH_3I decrease rapidly with height and are nearly twice as large in the NH at the surface during both missions. The greatest difference in CH_3I occurs between 1–4 km. The interhemispheric

(a) Ozone

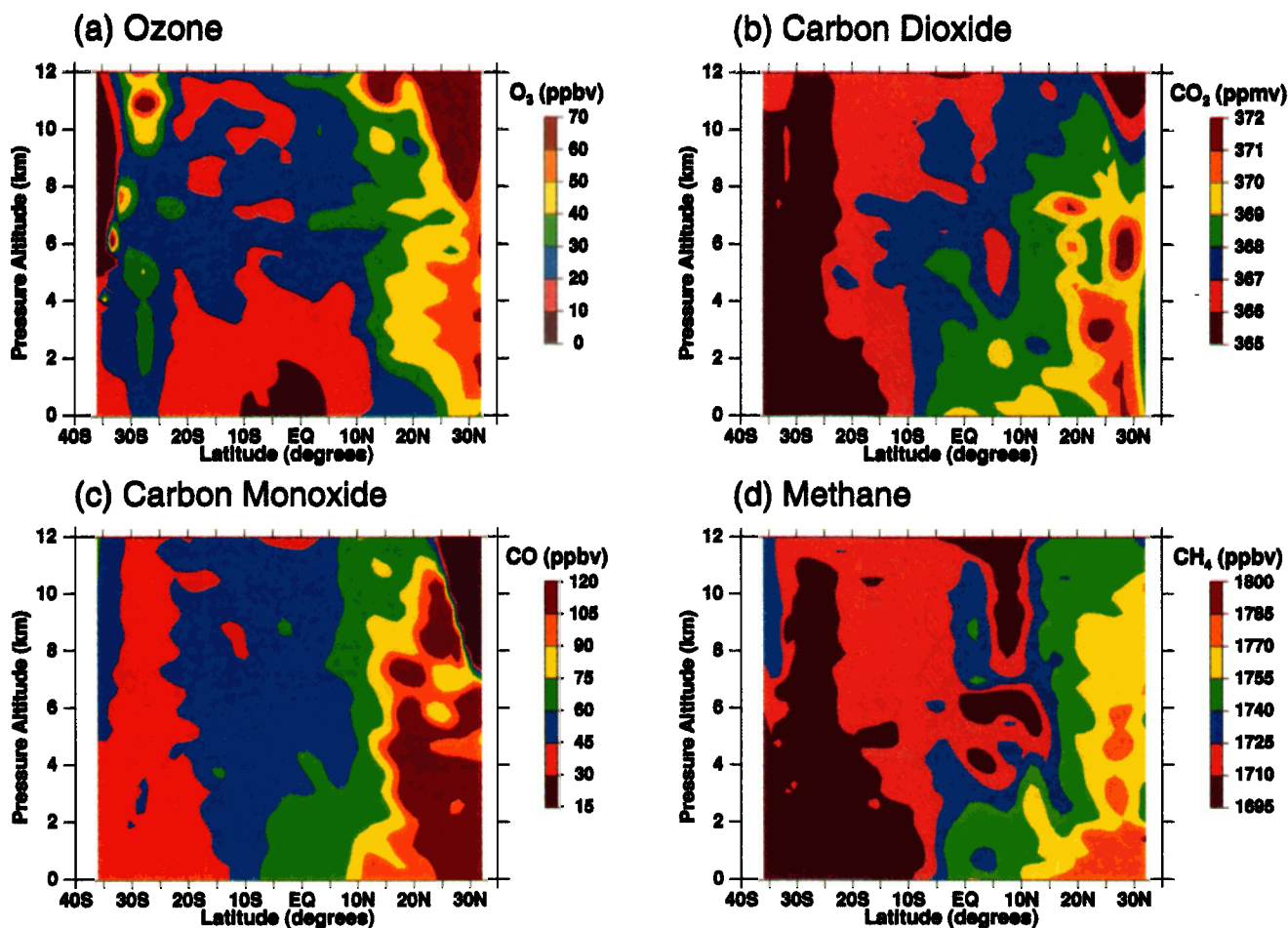## (b) Carbon Dioxide

(c) Carbon Monoxide

(d) Methane

Plate 5. Composite latitudinal cross sections of (a) ozone, (b) carbon dioxide, (c) carbon monoxide, and (d) methane measured from all flights of the DC-8 and P-3B in the central Pacific during PEM-Tropics B. The data are averaged over 4° of latitude and 0.5 km. The interpolated fraction of the plot was largest for CH_4 at 23%. The interpolated fraction of plots of the other species was 14% for CO and O_3 and 16% for CO_2.

gradient is reversed between missions. CH_3I in the NH is about 0.1 pptv greater during PTA than during PTB, consistent with less convective lifting in the NH during PTB. Enhancement of CH_3I at these altitudes in the SH during PTB is about 0.05 pptv, a difference that is only half as large as the NH enhancement during PTA, but probably equally significant because surface concentrations in the SH were also only half as large.

During PTB the large amount of SH convection resulted in elevated upper tropospheric H_2O and new particle production, as well as elevated CH_3I and a vertically mixed O_3 profile in the SH tropics. Relative humidity at all altitudes in the SH during PTB (Figure 5d) indicates that water vapor is greater in the SH than in the NH tropical Pacific. Particle nucleation during PTA was found to correspond with cloud-processed air at high altitudes, associated with elevated CH_3I and relative humidity [*Clarke et al.*, 1999]. Plate 7d shows the median profile and hemispheric differences in ultrafine particle concentrations between PTA and PTB. Ultrafine particle concentrations, which represent new particle formation, are much greater at all altitudes during PTB than during PTA, and are particularly large at high altitude. Although this is true in both hemispheres, it is particularly striking in the SH where there was more convective activity. This coincides with larger median relative humidities (Figure 5d). Elevated ultrafine particle concentrations

coincide with observations by differential absorbtion lidar [*Browell et al.*, this issue] of fewer aerosols in the SH than in the NH during PTB. This may represent reduced particle surface area, an additional requirement for new particle formation contrasting with the larger aerosol load observed in the SH during PTA by *Browell et al.* [1999].

6. Significance of Results

During the PTB mission in the central Pacific, northeasterly prevailing winds below 4 km (~600 hPa) near the equator in both hemispheres (Figure 1d) permit the large-scale transport of photochemically aged NH air across the equator. The equatorial region between ITCZ branches acts as an effective interhemispheric mixing region. This boundary between NH and SH air masses is spatially and temporally transient. Chemical gradients in the lower troposphere depend on the degree of surface convergence, with a larger chemical gradient coincident with more consistent surface convergence between northeasterly and southeasterly trade winds in the SH. Prevailing northeasterly flow and weaker surface convergence at the northern branch of the ITCZ generally allow NH air to pass across the equator into the geographical SH. Median near-surface concentrations of CO, CH_4, CO_2, C_2H_2, and C_2Cl_4
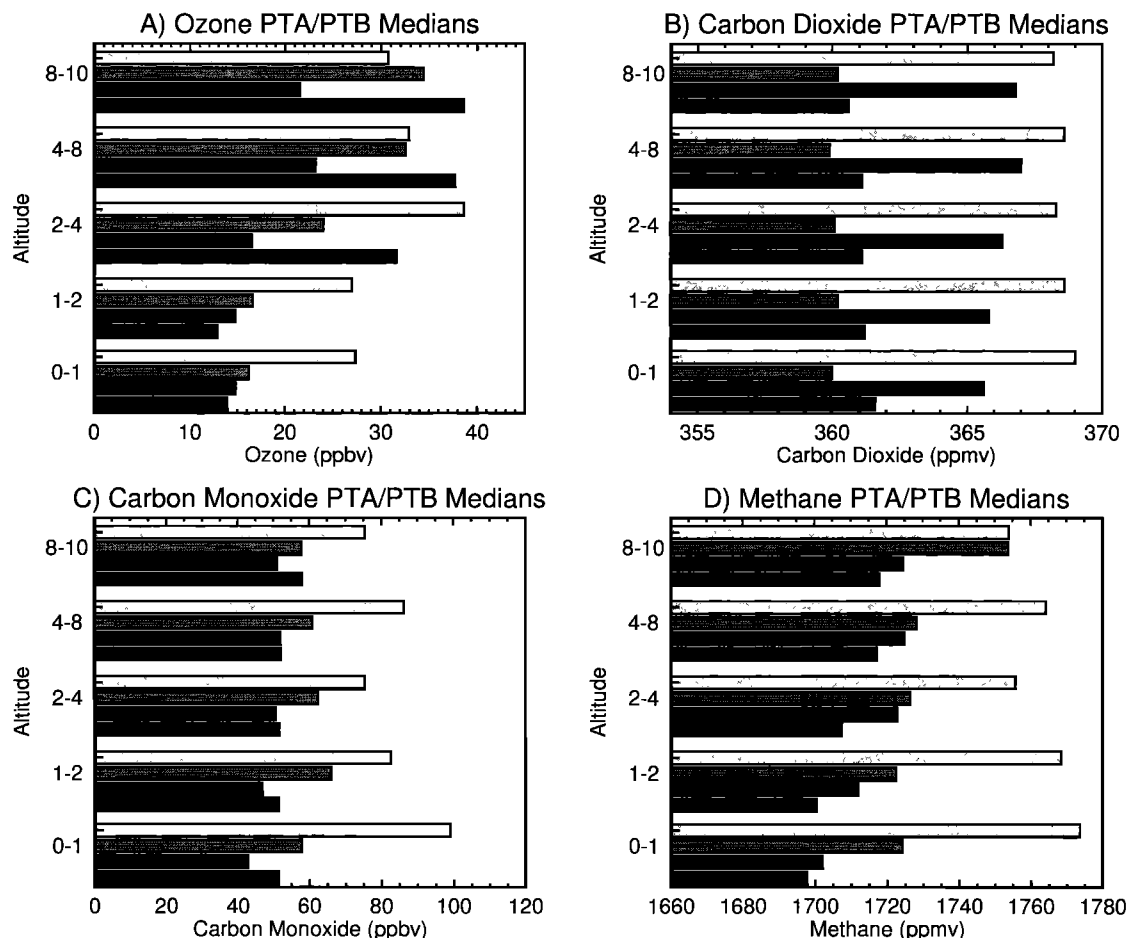
Figure 6. Vertical profiles of median values for (a) ozone, (b) carbon dioxide, (c) carbon monoxide, and (d) methane during PEM-Tropics B and PEM-Tropics A. The gray scale value is lightest for NH-PTB, medium gray for NH-PTA, dark gray for SH-PTB, and black for SH-PTA. The shading is the same for each altitude.

between branches of the ITCZ are significantly greater than those typical of the tropical SH during this time of year.

Pronounced vertical wind shear in the central Pacific causes the tropospheric dynamical and chemical boundary between hemispheres to be altitude-dependent. The layer of wind shear extends between 4–7 km as shown in Figures 2 and 3 and by the moist Hadley circulation [*Hu et al.*, this issue]. Above this midtropospheric transition zone, NH flow is dominated by the enhanced southern branch of the subtropical jet and a persistent clockwise circulation located at 150°W at the equator. The center of this circulation moved westward during the PEM-Tropics B mission, but most aircraft sampling was done on the west side of the circulation where the prevailing winds and persistent flow anomaly were southwesterly across the equator in the upper troposphere. Because high-altitude air most often was transported from the SH to NH during the PTB, median concentrations of most tracers at upper levels in the equatorial region are more representative of the SH.

A comparison of cross-ITCZ chemical tracer gradients between PEM-Tropics missions A and B shows that interhemispheric chemical gradients are larger during PTB, but sharper during PTA. For example, the interhemispheric CO_2 gradient at the surface is 2–3 ppm per 10 degrees of latitude, centered on 11°N, during PTA, while it is 3–5 ppm per 10 degrees, centered on 9°S, during PTB. Much of this difference can be

explained by the seasonal difference in chemical tracer source strength and transport dynamics. Because the double ITCZ structure is common during March and April, this is the optimum time of year for low-altitude transport of NH polluted air across the equator, particularly in the central Pacific. This transport also is favored during cold-phase ENSO events because of increased strength in the northeasterly trade winds and decreased surface convergence in the NH. Chemical measurements during PEM-Tropics B may represent an upper bound on the influence of NH polluted air near the surface in the SH tropics.

Although convection associated with the ITCZ typically is deep, *Gregory et al.* [1999] found that the ITCZ during PTA was a boundary between hemispheric air masses only at low altitudes. Although less clearly defined and spatially persistent, we find that this is also true during PTB. We note that persistent convective regions are most effective as barriers to horizontal transport where there are converging winds. At higher altitudes where the winds diverge, higher wind speeds associated with the prevailing winds cause more consistent, large-scale zonal and meridional horizontal transport. Convergence between winds originating at NH midlatitudes and the SH equatorial region in the shear layer of the middle troposphere coincides with a sharp gradient in chemical tracers in the NH that is not associated with the ITCZ. This indicates that con-
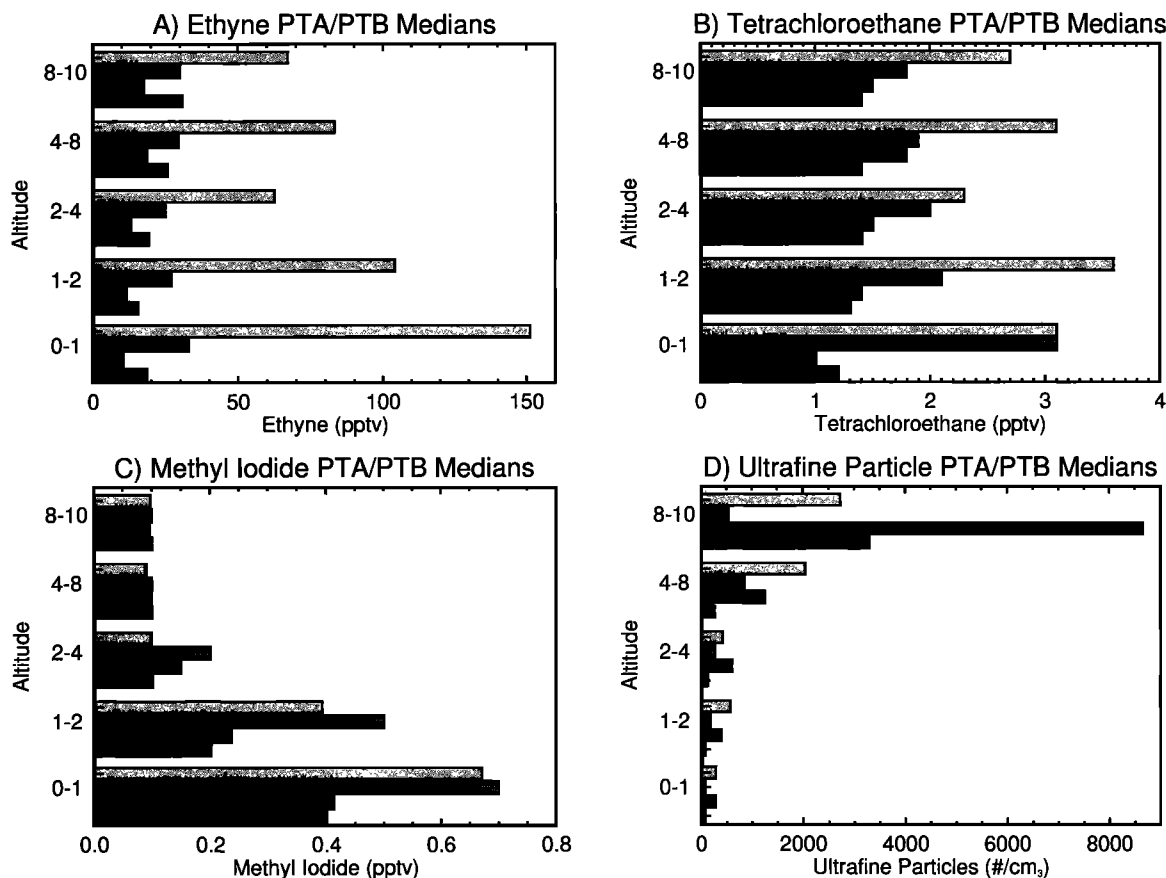
Figure 7. As in Figure 6, except that medians for PTA and PTB are shown for (a) ethyne, (b) tetra-chloro-ethylene, (c) methyl iodide, and (d) ultrafine particles.

verging winds that do not occur at the surface and are not associated with convection can also be effective as meridional transport barriers.

References

Barnett, T. P., M. Latif, E. Kirk, E. Roeckner, On ENSO physics, *J. Climate*, 4, 487–515, 1991.

Bergamaschi, P., D. C. Lowe, M. R. Manning, R. Moss, T. Bromley,

and T. S. Clarkson, Transects of atmospheric CO, CH_4, and their isotopic composition across the Pacific: Shipboard measurements and validation of inverse models, *J. Geophys. Res.*, 106(D8), 7993–8011, 2001.

Blake, N. J., et al., Influence of southern hemispheric biomass burning on midtropospheric distributions of nonmethane hydrocarbons and selected halocarbons over the remote South Pacific, *J. Geophys. Res.*, 104(D13), 16,213–16,232, 1999.

Blake, N. J., et al., Large-scale latitudinal and vertical distributions of NMHCs and selected halocarbons in the troposphere over the Pacific Ocean during the March–April 1999 Pacific Exploratory Mission (PEM-Tropics B), *J. Geophys. Res.*, this issue.

Browell, E. V., et al., Large-scale air mass characteristics observed over the remote tropical Pacific Ocean during March–April 1999: Results from PEM-Tropics B field experiment, *J. Geophys. Res.*, this issue.

Clarke, A. D., et al., Nucleation in the equatorial free troposphere: Favorable environments during PEM-Tropics A, *J. Geophys. Res.*, 104(D5), 5735–5744, 1999.

Cohan, D. S., M. G. Schultz, D. J. Jacob, B. G. Heikes, and D. R. Blake, Convective injection and photochemical decay of peroxides in the tropical upper troposphere: Methyl iodide as a tracer of marine convection, *J. Geophys. Res.*, 104(D5), 5717–5724, 1999.

Fuelberg, H. E., R. E. Newell, S. P. Longmore, Y. Zhu, D. J. Westberg, E. V. Browell, D. R. Blake, G. L. Gregory, and G. W. Sachse, A meteorological overview of the Pacific Exploratory Mission (PEM) Tropics period, *J. Geophys. Res.*, 104(D5), 5585–5622, 1999.

Fuelberg, H. E., R. E. Newell, D. J. Westberg, J. C. Maloney, J. R. Hannan, B. D. Martin, M. A. Avery, and Y. Zhu, A meteorological overview of the second Pacific Exploratory Mission in the tropics, *J. Geophys. Res.*, this issue.

Gregory, G. L., et al., Chemical characteristics of Pacific tropospheric air in the region of the Intertropical Convergence Zone and South Pacific Convergence Zone, *J. Geophys. Res.*, 104(D5), 5677–5696, 1999.

Hoell, J. M., D. D. Davis, D. J. Jacob, M. O. Rodgers, R. E. Newell, H. E. Fuelberg, R. J. McNeal, J. L. Raper, and R. J. Bendura, Pacific Exploratory Mission in the tropical Pacific: PEM-Tropics A, August–September 1996, *J. Geophys. Res.*, *104*(D5), 5567–5584, 1999.

Hu, Y., R. E. Newell, and Y. Zhu, Mean moist circulation for PEM-Tropics missions, *J. Geophys. Res.*, this issue.

Karoly, D. J., D. G. Vincent, and J. M. Schrage, General circulation, in *Meteorology of the Southern Hemisphere*, chap. 2, pp. 47–85, Am. Meteorol. Soc., Boston, Mass., 1998.

Kiladis, G. N., and K. C. Mo, Interannual and interseasonal variability in the Southern Hemisphere, in *Meteorology of the Southern Hemisphere*, chap. 8, pp. 307–336, Am. Meteorol. Soc., Boston, Mass., 1998.

Maloney, J. C., H. E. Fuelberg, M. A. Avery, D. R. Blake, B. G. Heikes, G. W. Sachse, S. T. Sandholm, H. Singh, and R. W. Talbot, Chemical characteristics of air from different source regions during the second Pacific Exploratory Mission in the tropics (PEM-Tropics B), *J. Geophys. Res.*, this issue.

Olson, J. R., et al., Seasonal differences in the photochemistry of the South Pacific: A comparison of observations and model results from PEM-Tropics A and B, *J. Geophys. Res.*, this issue.

Raper, J. L., M. M. Kleb, D. J. Jacob, D. D. Davis, R. E. Newell, H. E. Fuelberg, R. J. Bendura, J. M. Hoell, and R. J. McNeal, Pacific Exploratory Mission in the tropical Pacific: PEM-Tropics B, March–April 1999, *J. Geophys. Res.*, this issue.

Seinfeld, J. H., and S. N. Pandis, *Atmospheric Chemistry and Physics*, John Wiley, New York, 1998.

Shapiro, M. A., H. Wernli, N. A. Bond, and R. Langland, The influence of the 1997–1999 ENSO on extratropical baroclinic life cycles over the eastern North Pacific, *Q. J. R. Meteorol. Soc.*, *126*, 1–20, 2000.

Vay, S. A., B. E. Anderson, T. J. Conway, G. W. Sachse, J. E. Collins Jr., D. R. Blake, and D. J. Westberg, Airborne observations of the tropospheric CO_2 distribution and its controlling factors over the South Pacific Basin, *J. Geophys. Res.*, *104*(D5), 5663–5676, 1999.

Waliser, D. E., and C. Gautier, A satellite-derived climatology of the ITCZ, *J. Clim.*, *6*, 2162–2174, 1993.

B. E. Anderson, M. A. Avery, G. W. Sachse, S. A. Vay, and D. J. Westberg, Chemistry and Dynamics, NASA Langley Research Center, Hampton, VA 23681, USA.

D. R. Blake, Department of Chemistry, University of California, Irvine, CA 92717, USA.

H. E. Fuelberg, Department of Meteorology, Florida State University, Tallahassee, FL 32306, USA.

R. E. Newell, Department of Earth, Atmospheric, and Planetary Sciences, Massachusetts Institute of Technology, Cambridge, MA 02139, USA.